A Novel Extended Desired Compensation Adaptive Law for High-Speed Pick-and-Throw with PKMs

Ghina Hassan, Ahmed Chemori, Marc Gouttefarde, Maher El Rafei, Clovis Francis, Pierre-Elie Hervé, Damien Sallé

14th IFAC International Workshop on
Adaptation and Learning in Control and Signal Processing
June 29 - July 1, 2022. Casablanca, Morocco

A Novel Extended Desired Compensation Adaptive Law for High-Speed Pick-and-Throw with PKMs

G. Hassan [*,**] **A. Chemori** [*] **M. Gouttefarde** [*] **M. El Rafei** [**] **C. Francis** [**]
P.E. Hervé [***] **D. Sallé** [***]

[*] *LIRMM, Univ Montpellier, CNRS, Montpellier, France (e-mail: ghina.hassan, ahmed.chemori, marc.gouttefarde@lirmm.fr)*
[**] *CRSI, Lebanese University, Faculty of Engineering, Beirut, Lebanon (e-mail: maher.elrafei, cfrancis@ul.edu.lb)*
[***] *TECNALIA, Basque Research and Technology Alliance (BRTA), San Sebastian, Spain (e-mail: pierre-elie.herve, damien.salle@tecnalia.com)*

Abstract: This paper focuses on the development of a new revised Desired Compensation Adaptive Law (DCAL). DCAL is a model-based adaptive control strategy consisting of three main parts: (i) an adaptive feedforward term, (ii) a linear PD feedback term, and (iii) a nonlinear compensation term. In order to deal with highly nonlinear dynamic systems characterized by their abundant uncertainties and parameters variations, we propose to revise the original DCAL control law by adopting adaptive feedback gains depending on the system state errors. Besides, DCAL controller is known for its robustness against measurement noise thanks to its desired compensation design, but a large amount of external disturbances are still not compensated by such a design. Therefore, the proposed DCAL with adaptive gains (DCAL-AG) is extended with a sliding-based term to further improve its robustness and the overall performance. A model-based robust adaptive feedback controller appropriate to the control of nonlinear systems in real-time applications is thereby obtained. To demonstrate the improvements brought by the proposed control strategy, numerical simulations have been conducted on a Delta-link parallel robot named T3KR in a "Pick-and-Throw" application task at different operating conditions.

Keywords: Robust DCAL, adaptive gains, parallel kinematic manipulator, pick-and-throw, numerical simulations.

1. INTRODUCTION

Over the last decades, parallel kinematic manipulators (PKMs) have provided a part of industrial and research resources. These manipulators are characterized by their rigidity, high precision, high dynamics and lightness (Merlet, 2005). Nevertheless, PKMs inherit the complexity of their closed kinematic chain structure where two or more kinematic chains connect the moving plate to the fixed base. In addition, they are characterized by high uncertainties, parameter variations, external disturbances (Pi and Wang, 2011) and nonlinear dynamics, especially in high-acceleration applications (Natal et al., 2014). As a result, the design of sophisticated control strategies for these kind of manipulators is a challenging task.

In the literature, several control schemes have been proposed aiming to accurately drive PKMs. On the one hand, the kinematic controllers, known by non-model-based controllers, can achieve acceptable performance as long as the operating conditions do not change (Saied et al., 2019). Nevertheless, as mentioned above, PKMs are nonlinear dynamic systems, subject to uncertainties and time-varying parameters, thus, a kinematic controller may deteriorate the performance and lead to undesirable behavior. On the other hand, research works show that designing a controller that is partially or fully rich in knowledge about the system dynamics can improve tracking performance by compensating for the system nonlinearities (Codourey, 1998; Shang et al., 2009). However, these types of controllers require an accurate dynamic model of the robotic system which is a difficult task or even an impossible one. Therefore, the need for adaptive control schemes arises. Model-based adaptive controllers can online adjust the dynamic parameters, leading to an adequate compensation of dynamic nonlinearities and possible parameter variations and uncertainties of PKMs (Bennehar et al., 2017, 2015, 2018). The Desired Compensation Adaptive Law (DCAL), developed by Sadegh et al. in 1990 (Sadegh and Horowitz, 1990), has been applied, to drive a six-degrees-of-freedom (6-DOF) PKM named *Hexaglide*, for the first time in (Honegger et al., 1997). It has shown a good tracking performance, while estimating in real-time all the inertial and friction parameters of the manipulator. Both in the control and in the adaptation laws, this controller uses the desired trajectories instead of the measured ones, which can explain its effectiveness. An extended version of DCAL has been proposed in (Bennehar et al., 2014) to enhance accuracy of PKMs.

Thanks to their above advantages, a very wide range of applications benefit from PKMs. Recently, PKMs have been used as a robotic solution for selective waste sorting (BHS, 2018). Such an application is considered as a difficult task for PKMs, since the manipulator has to handle different types of objects with different physical parameters, that may often be unknown or uncertain. Therefore, model-based adaptive schemes, characterized by dynamic parameter identification in an online algorithm, are the most appropriate control solutions for such kind of applications. For instance, the aforementioned DCAL may be a good candidate, thanks to its simple structure easy

to implement, its real-time estimation of the model parameters, and its robustness against measurement noise.
Nevertheless, DCAL is characterized by constant linear feedback gains. As known, static feedback control algorithms can provide good performance only in nominal steady state and when no changes in operating conditions occur. However, it has been shown that control methods with adaptive dynamic feedback gains can counteract external disturbances and accommodate the variations in dynamic parameters (Gholami et al., 2009; Tijjani et al., 2020; Escorcia-Hernández, 2020).
In this paper, we aim to deal with uncertain and unknown objects in a Pick-and-Throw application using a PKM. Accordingly, for this task, online estimation of dynamic parameters is required. Therefore, we propose to exploit the advantages of the real-time estimation of the model parameters provided by DCAL and the corrective action produced by an adequate adaptation law for the feedback gains. In addition, to better counteract the external disturbances, we propose to extend the resulting controller by a nonlinear sliding-based term computed from the signum of the system state errors. The addition of this robustness related term will accommodate for the lack of robustness and can improve the overall tracking performance. In a real-time implementation, the discontinuous signum function may be replaced by a continuous sigmoid function to avoid chattering. For the adaptation law of the feedback gains, we propose to use the algorithm developed by (Plestan et al., 2010). It is a continuous adaptation law that ensures a non-overestimation of the gains with respect to the perturbations. Numerical simulations have been conducted in different scenarios of a Pick-and-Throw application in order to investigate the enhancement and the robustness brought by the proposed control scheme.
The rest of the paper is organized as follows: The proposed control strategy is introduced in Section 2. The description and modeling of T3KR parallel robot are provided in Section 3. In Section 4, the obtained numerical simulation results in different scenarios are discussed, and finally, some concluding remarks are drawn in Section 5.

2. PROPOSED CONTRIBUTION: ROBUST DCAL WITH ADAPTIVE FEEDBACK GAINS

The dynamics of a *m*-DOF kinematic manipulator controlled by *n* actuators can be described in joint space as follows (Siciliano et al., 2010):

$$M(q)\ddot{q}+C(q,\dot{q})\dot{q}+G(q)+\Gamma_d(t)=\Gamma(t) \tag{1}$$

where $M(q)\in\mathbb{R}^{n\times n}$ is the total mass and inertia matrix of the robot, $C(q,\dot{q})\in\mathbb{R}^{n\times n}$ denotes the Coriolis and centrifugal forces matrix, $G(q)\in\mathbb{R}^n$ is the gravitational forces vector. $q,\dot{q},\ddot{q}\in\mathbb{R}^n$ are the joint position, velocity and acceleration vectors, respectively. The vector $\Gamma_d(t)\in\mathbb{R}^n$ gathers a large class of nonlinear disturbances (i.e. external disturbances, unknown friction effects, unmodeled phenomena, etc.) and $\Gamma(t)\in\mathbb{R}^n$ is the control input vector.
According to (Craig et al., 1987), the manipulator dynamic model is characterized by its linearity with respect to dynamic parameters such as inertia and masses. All constant parameters in the dynamic model are considered as coefficients of known functions (linear and nonlinear) of $q,\dot{q},\ddot{q}$. The external disturbances $\Gamma_d(t)$ are excluded from the linear reformulation of the dynamics since they are not modeled and cannot be written in a linear form of the parameters. Therefore, (1) can be rewritten as follows:

$$M(q)\ddot{q}+C(q,\dot{q})\dot{q}+G(q)+\Gamma_d(t)=\mathrm{W}(q,\dot{q},\ddot{q})\Phi(t)+\Gamma_d(t) \tag{2}$$

where $\mathrm{W}(q,\dot{q},\ddot{q})\in\mathbb{R}^{n\times p}$ is called the regression matrix and is formed by known nonlinear functions of $q,\dot{q},\ddot{q}$. The vector $\Phi\in\mathbb{R}^p$ gathers the geometrical and dynamic parameters of the robot. In the sequel, a background on the standard DCAL will be provided. Then, the proposed control approach will be detailed.

2.1 General overview of DCAL control strategy

DCAL is a model-based adaptive control scheme developed by Sadegh et al. in 1990 (Sadegh and Horowitz, 1990). Its control law can be split up into three main parts: (i) a model-based adaptive feedforward part, (ii) a linear feedback part, and (iii) an additional nonlinear feedback function. The relevance of DCAL lies in both the control and adaptation laws which use the desired joint trajectories instead of the measured ones. This is of great importance since the computational time may be significantly reduced and the effect of measurement noises is eliminated. The additional nonlinear term aims to accommodate for the errors resulting from using the desired states instead of the measured ones. The joint-space control law of DCAL is then expressed as follows (Sadegh and Horowitz, 1990):

$$\Gamma_{DCAL}=W(q_d,\dot{q}_d,\ddot{q}_d)\hat{\Phi}(t)+\Lambda_p\,e(t)+\Lambda_v\,e_v(t)+\sigma\|e(t)\|^2\,e_v(t) \tag{3}$$

where $e(t)=q_d(t)-q(t)$ is the joint position tracking error, with $q_d(t)\in\mathbb{R}^n$ is the vector of desired joint positions and $q(t)\in\mathbb{R}^n$ is the vector of measured ones. $e_v(t)=\dot{e}(t)+\lambda e(t)$ is the combined position-velocity tracking error, $\lambda\in\mathbb{R}^+$ is a positive design gain. Λ_P, $\Lambda_v\in\mathbb{R}^{n\times n}$ are positive-definite gain matrices, usually chosen diagonal. $W(q_d,\dot{q}_d,\ddot{q}_d)\in\mathbb{R}^{n\times p}$ is the regressor matrix function depending on desired joint positions, velocities and accelerations. $\hat{\Phi}(t)\in\mathbb{R}^{n\times p}$ is an online estimation of the unknown parameters vector Φ, and $\sigma\in\mathbb{R}^+$ is a positive design control parameter.
The time-evolution of the estimated parameters $\hat{\Phi}(t)$ in (3) is expressed by the following adaptation law:

$$\dot{\hat{\Phi}}(t)=KW^T(q_d,\dot{q}_d,\ddot{q}_d)e_v(t) \tag{4}$$

where $K\in\mathbb{R}^{p\times p}$ is a diagonal positive-definite adaptation gain matrix. As it can be seen, the regressor W in the adaptation law (4) is also evaluated based on the desired trajectories instead of the measurements.

2.2 Proposed robust DCAL with adaptive gains

Despite the efficiency of the standard DCAL, it exhibits a lack of performance due to the static linear feedback gains and the potential presence of external disturbances not compensated by the control law. To significantly improve the overall performance of such a controller, we first propose to replace the linear feedback term with an adaptive one where the gains are adjusted online according to the system state errors. Second, to further improve its robustness against disturbances, a sliding-based term depending on the combined error is added. The resulting expression of the proposed control law can be written as follows:

$$\begin{aligned}\Gamma_{RDCAL-AG}=&W(q_d,\dot{q}_d,\ddot{q}_d)\hat{\Phi}(t)+\Lambda_p(t)\,e(t)\\&+\Lambda_v(t)\,e_v(t)+\sigma\|e(t)\|^2\,e_v(t)+\beta sgn(e_v(t))\end{aligned} \tag{5}$$

where $\beta\in\mathbb{R}^{n\times n}$ is a constant positive-definite gain matrix. $\Lambda_p(t)$ and $\Lambda_v(t)\in\mathbb{R}^{n\times n}$ are time-varying gains matrices. One

interesting choice of the time evolution of the adaptive feedback gain matrices can be formulated based on the mechanism proposed in (Plestan et al., 2010) as follows:

$$\Lambda_p(t) = \bar{\Lambda}_p|\eta_p| + \Lambda_{pm}, \quad \dot{\eta}_p = \tanh(e) - \eta_p \tag{6}$$

$$\Lambda_v(t) = \bar{\Lambda}_v|\eta_v| + \Lambda_{vm}, \quad \dot{\eta}_v = \tanh(e_v) - \eta_v \tag{11}$$

Where $\bar{\Lambda}_p$ and $\bar{\Lambda}_v \in \mathbb{R}^{n\times n}$ are positive-definite constant matrices, chosen to be diagonal. While Λ_{pm} and $\Lambda_{vm} \in \mathbb{R}^{n\times n}$ are other positive-definite diagonal matrices denoting the minimum value for each adaptive gain. η_p and $\eta_v \in \mathbb{R}^n$ are nonlinear functions depending on the tracking error e and the combined tracking error e_v, respectively. For more details on this adaptation law and the stability analysis using it in a robust control law, the reader can refer to Escorcia-Hernández (2020).
It is worth to note that when the tracking error increases, the adaptive gains of the proposed control law produce a corrective action to reduce this large tracking error. Once it decreases, the adopted strategy begins to reduce the control action and adjusts the gains to avoid oscillations and sufficiently counteract the current uncertainties and disturbances. When it comes to the estimation of unknown dynamic parameters, the same adaptation law (4) is adopted for the proposed controller. Therefore, this new control technique inherits the advantages of the original DCAL in terms of noise measurement reduction and low computational time.

3. T3KR ROBOT: DESCRIPTION, MODELLING AND CONTROL APPLICATION

3.1 Description and kinematics of T3KR robot

T3KR, shown in Fig. 1, is a rigid-link parallel robot designed within the framework of a cooperation between SATT AxLR, Tecnalia and LIRMM. It features an economical footprint with five DOF. Three translational motions along x, y and z axes, and one rotational motion, ψ, of the moving platform around the vertical z axis, are generated by the four main actuators placed on the fixed base. These motors are connected to the moving platform by four kinematic chains. Each of the kinematic chains is formed by a main actuator, a movable rearm and a forearm composed of two parallel rods (cf. Fig. 1). In addition, a rotational movement, ϕ, of the robot end-effector around the z axis, is provided by a further actuator fixed at the mobile platform. It should be noted that the ψ rotation of the platform is kept at zero for all the proposed scenarios. It is worth to emphasize the innovative point of this robot: if the last coordinate is changed, the tool control point (TCP) does not move; in fact the rotation of the platform is a parallelogram mechanism movement, and the TCP is on the neutral axis of the mechanism. In our study, we are concerned only with the control of the parallel Delta-like positioning structure. Consider the vector $X = [x, y, z, \psi]^T$ as the Cartesian position and orientation of the end-effector, and the vector $q = [q_1, q_2, q_3, q_4]^T$ as the actuated joint positions. The differential kinematic relationship between the Cartesian and joint velocities can be expressed, using the Jacobian matrix J, as follows: $\dot{X} = J\dot{q}$, where $\dot{X}$ and $\dot{q}$ are the Cartesian and joint velocities, respectively.

3.2 Dynamics of T3KR parallel robot

Based on the virtual work principle, the dynamics of T3KR robot can be elaborated (Codourey, 1998). The following assumptions are considered to simplify the PKM dynamic model

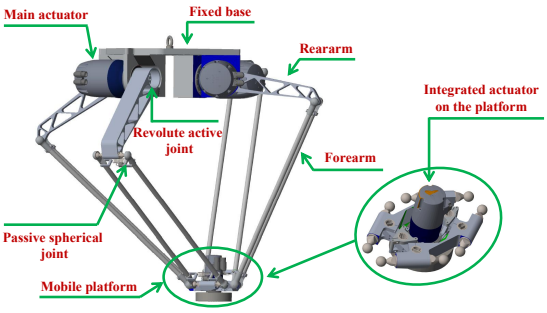

Fig. 1. A CAD view of the T3KR parallel robot with its main components.

while maintaining its relevance:
Assumption 1: *The masses of the forearms are smaller than the others parts of the robot, hence their inertia is neglected.*
Assumption 2: *The mass of each forearm is divided into two pointwise masses located at both extremities of the forearms.*
Assumption 3: *Both dry and viscous frictions in all passive and active joints are neglected.*

The dynamics of T3KR robot can be reduced to the analysis of the dynamics of its moving platform and those of the actuators with their corresponding rearms and forearms. Regarding the moving platform's dynamics, one can consider two kinds of forces acting on it produced by the gravity and Cartesian accelerations. The contributions of these two forces to actuator torques can be expressed as follows:

$$\Gamma_{G_{tp}} = -J^T M_{tp} G, \quad \Gamma_{F_{tp}} = J^T M_{tp} \ddot{X} \tag{7}$$

where $M_{tp} = diag\{m_{tp}, m_{tp}, m_{tp}, i_{tp}\}$ with $m_{tp} = m_n + 4\frac{m_f}{2}$ is the total mass of the mobile platform including the mass of the actuator integrated on the platform, the payload handled by the end-effector and the four half masses of the forearms. i_{tp} is the total inertia of the platform. $G \in \mathbb{R}^4$ is the gravity vector ($G = [0, 0, g, 0]^T$, being $g = 9.81\, m/s^2$ the gravity acceleration). $\ddot{X} \in \mathbb{R}^4$ denotes the Cartesian acceleration vector.
Regarding the dynamics of the rearms, three torques acting on them can be distinguished : (i) the contribution of the actuators input torque $\Gamma \in \mathbb{R}^4$, (ii) the torque due to the gravitational forces acting on the rearms $\Gamma_{G_{arm}} \in \mathbb{R}^4$, and (iii) the inertial contribution torque produced by the joint acceleration on the rearms $\Gamma_{arm} \in \mathbb{R}^4$:

$$\Gamma_{G_{arm}} = -g\, M_r\, Cos(q), \quad \Gamma_{arm} = I_{arm}\ddot{q} \tag{8}$$

where $M_r = diag\{m_{req}, m_{req}, m_{req}, m_{req}\}$ with $m_{req} = m_r L_{rG} + L\frac{m_f}{2}$, m_r is the mass of each rearm, l_{rG} is the distance from the axis of rotation of each rearm to its center of gravity, while L is the complete length of each rearm. $Cos(q) = [cos(q_1), cos(q_2), cos(q_3), cos(q_4)]^T$ and $\ddot{q} \in \mathbb{R}^4$ represents the accelerations in joint space. $I_{arm} \in \mathbb{R}^{4x4}$ is a diagonal inertia matrix that gathers the actuators inertia, the reamarms inertia and the inertial contribution of the forearms with respect to the actuators' rotation axes using Assumption 2.
Following (Codourey, 1998), the sum of all non-inertial forces should be equal to the sum of all inertial forces, then the inverse dynamic model of T3KR robot can be expressed in terms of the joint coordinates as follows:

$$M(q)\ddot{q} + C(q,\dot{q})\dot{q} + G(q) = \Gamma(t) \tag{9}$$

where $M(q) = I_{arm} + J^T M_{tp} J$ denotes the total mass and inertia matrix of the robot, $C(q,\dot{q})\dot{q} = J^T M_{tp}\dot{J}$ denotes the Coriolis

Table 1. Summary of the main geometric and dynamic parameters of T3KR robot.

Parameter	Value	Parameter	Value
Rear-arm length (L)	400 mm	Nacelle mass (m_n)	5.68 Kg
Forearm length (l)	900 mm	Actuator inertia (I_{act})	0.000969 Kg.m^2
Rear-arm mass (m_r)	3.28 Kg	Rear-arm inertia (I_r)	0.173723 Kg.m^2
Forearm mass (m_f)	0.8 Kg		

and centrifugal forces matrix, with $\dot{J}$ being the time derivative of J, $G(q) = -\Gamma_{G_{arm}} - \Gamma_{G_{tp}}$ represents the gravitational forces vector, and $\Gamma(t)$ is the control input vector. For more details on the development of PKM dynamic model, the reader can refer to Bennehar et al. (2018). If the external disturbances are considered, the dynamic model of T3KR robot can be rewritten as in (1). The main geometric and dynamic parameters of T3KR parallel robot are summarized in Table 1.

3.3 Control application

Our main objective is to use the proposed RDCAL-AG controller in a Pick-and-Throw selective sorting task. In such an application, the robot is subject to payload variations since the mass of the mobile platform (including the payload) may vary continuously depending on the object being handled. Accordingly, in our case study, the adaptation algorithm of the parameters estimation only accounts for the mass of the moving platform, including the payload, while taking advantage of the known dynamic parameters of the other robot parts. Therefore, the dynamic model of T3KR (9) with the consideration of the external disturbances can be reformulated according to (2) as follows:

$$M(q)\ddot{q} + C(q,\dot{q})\dot{q} + G(q) + \Gamma_d(t) = W_u(q,\dot{q},\ddot{q})\Phi_u + I_{arm}\ddot{q} + gM_rCos(q) + \Gamma_d(t) \tag{10}$$

The partial regression matrix W_u only accounts for the dynamics of the mobile platform and is given by:

$$W_u = J^T(J\ddot{q} + \dot{J}\dot{q} + G) = J^T(\ddot{X} + G) \tag{11}$$

Φ_u is the mass m_{tp} of the mobile platform including the mass of the carried payload, $\Phi_u = m_{tp}$. Therefore, the original DCAL and the proposed control law are reformulated as follows:

$$\Gamma_{DCAL} = W_u(q_d,\dot{q}_d,\ddot{q}_d)\hat{\Phi}_u + I_{arm}\ddot{q}_d + gM_rCos(q_d) + \Lambda_p\, e(t) + \Lambda_v\, e_v(t) + \sigma\|e(t)\|^2\, e_v(t) \tag{12}$$

$$\Gamma_{RDCAL-AG} = W_u(q_d,\dot{q}_d,\ddot{q}_d)\hat{\Phi}_u + I_{arm}\ddot{q}_d + gM_rCos(q_d) + \Lambda_p(t)\, e(t) + \Lambda_v(t)\, e_v(t) + \sigma\|e(t)\|^2\, e_v(t) + \beta sgn(e_v(t)) \tag{13}$$

where $\hat{\Phi}_u$ is the online estimation of Φ_u.

4. NUMERICAL SIMULATION RESULTS

In this section, the obtained simulation results of the proposed RDCAL-AG, the original DCAL and a model-based adaptive robust control from the literature are presented and discussed.

4.1 Implementation issues

Model-based adaptive RISE control: The RISE-based adaptive control, developed in (Bennehar et al., 2018), will be used for comparison purposes as it is a robust model-based adaptive controller. Its control law is expressed as follows:

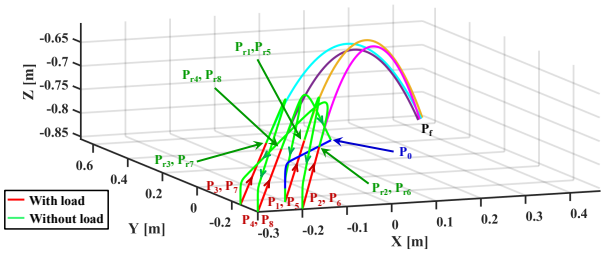

Fig. 2. 3D-view of the P&T reference trajectories of the robot (the red and green lines) with the ballistic motions of the thrown objects in Cartesian space.

$$\Gamma_{ARISE} = W_u(q_d,\dot{q}_d,\ddot{q}_d)\hat{\Phi}_u + I_{arm}\ddot{q}_d + gM_rCos(q_d) + (K_s+I)e_2(t) - (K_s+I)e_2(t_0) + \int_{t_0}^{t}[(K_s+I)\alpha_2 e_2(\sigma) + \beta sgn(e_2(\sigma))]d\sigma. \tag{14}$$

where $e_2(t) = \dot{e}(t) + \alpha_1 e(t)$ is the combined error. α_1, α_2, K_s and $\beta \in \mathbb{R}^{n\times n}$ are positive-definite, diagonal gain matrices, $I \in \mathbb{R}^{n\times n}$ is identity matrix, t_0 is the initial time and $sgn(.)$ is the sign function. n is equal to 4 in our case study. The standard PID controller will not be considered for comparison in this work because its performance has been shown in the literature to be less good than robust and model-based controllers Natal et al. (2014); Hassan et al. (2020).

Reference trajectories generation: The P&T reference trajectories, sketched in Fig. 2, are generated using a 3^{rd} order polynomial S-curve motion profile. In these trajectories, the robot has to pick and throw eight objects, located at different positions, towards a target position, $\mathbf{P}_f$, located outside of its workspace. The robot moves from the homing position $\mathbf{P}_0$ to the first pick position $\mathbf{P}_1$. After picking the 1^{st} object, the robot accelerates while moving along a straight line towards the release position $\mathbf{P}_{r_1}$ at which it throws the object towards the target position $\mathbf{P}_f$. Once released, the object follows its free-flight ballistic trajectory to $\mathbf{P}_f$ while the robot decelerates back to pick the second object. The same cyclic movement is repeated for the second, the third, and the fourth objects, located at $\mathbf{P}_2$, $\mathbf{P}_3$, and $\mathbf{P}_4$, respectively. After throwing the fourth object, the robot moves to $\mathbf{P}_5$, to pick the fifth object. The same throw motion is performed for the last fourth objects located at $\mathbf{P}_5$, $\mathbf{P}_6$, $\mathbf{P}_7$, and $\mathbf{P}_8$, respectively. After throwing the last object, the robot moves back to $\mathbf{P}_0$.

Performance Evaluation criteria: To evaluate the effectiveness of the proposed controller, a frequently used performance index, the Root Mean Square Error (*RMSE*) criterion, is adopted in our study. The *RMSE* for Cartesian translational positions $RMSET_C$ and joint positions $RMSE_J$ are expressed respectively as follows:

$$RMSET_C = \sqrt{\left(\frac{1}{N}\sum_{i=1}^{N}(e_x^2(i) + e_y^2(i) + e_z^2(i))\right)} \tag{15}$$

$$RMSE_J = \sqrt{\left(\frac{1}{N}\sum_{i=1}^{N}(e_{q_1}^2(i) + e_{q_2}^2(i) + e_{q_3}^2(i) + e_{q_4}^2(i))\right)} \tag{16}$$

where e_x, e_y and e_z are the Cartesian position tracking errors along the x, y and z *axes*, respectively. While e_{q_1}, e_{q_2}, e_{q_3} and e_{q_4} denote the joint position tracking errors, and N is the total number of samples.

Table 2. Summary of the tuned feedback gains.

Standard DCAL		Adaptive RISE		Proposed RDCAL-AG	
$\Lambda_p = 1135$	$\sigma = 4.5\times10^6$	$\alpha_1 = 150$	$\beta = 2.5$	$\Lambda_{pm} = 1135$	$\sigma = 4.5\times10^6$
$\Lambda_v = 22.7$	$K = 200$	$\alpha_2 = 0.3$	$K = 180$	$\bar{\Lambda}_p = 4\times10^7$	$\lambda = 100$
$\lambda = 100$		$K_s = 22$		$\Lambda_{vm} = 22.7$	$K = 300$
				$\bar{\Lambda}_v = 105$	$\beta = 2.5$

Table 3. Control performance evaluation

	$RMSET_C$[mm]		$RMSE_J$[deg]	
	S1	S2	S1	S2
Standard DCAL	0.0981	0.1252	0.0136	0.0149
Adaptive RISE	0.0888	0.0877	0.0090	0.0101
Porposed RDCAL-AG	0.0545	0.0629	0.0073	0.0074
Improvements w.r.t DCAL	44.4 %	49.7 %	46.3 %	50.3%
Improvements w.r.t ARISE	38.6 %	28.3 %	18.8 %	26.7%

Tuning the control gains: For the controllers tested on T3KR, the gains were adjusted by the trial-and-error method. For the proposed RDCAL-AG controller, we first set a high value for λ and minimum possible values for Λ_{pm} and Λ_{vm}. Then, the gains $\bar{\Lambda}_p$ and $\bar{\Lambda}_v$ were adjusted, either increasing or decreasing, until the best performance is obtained. The K gain, responsible for the parameters' estimation, is increased gradually till obtaining a good convergence of the mass of the platform. The σ gain is then increased to improve the overall performance while keeping the control input values away from saturation. Finally, the gain β, responsible for the robustness of the controller, is increased progressively in order to obtain better performance while maintaining low chattering input signals. The resulting gains values of the proposed controllers are summarized in Table 2. It is worth to note that the gain parameters are adjusted while respecting the actuators limits. In addition, for a fair comparison, the common parameters between the three tested controllers on T3KR are set to be the same.

4.2 Obtained simulations results

Numerical simulations have been conducted on T3KR robot in a P&T task to demonstrate the performance of the proposed controller. A comparison between the standard DCAL, the RISE-based adaptive control and the proposed controller has been established, in Matlab/Simulink environment with a fixed step solver equal to 0.4 ms, using the P&T reference trajectories illustrated in Fig. 2. Two main scenarios have been conducted in this demonstration: 1) *scenario 1*: robustness towards payload changes, 2) *scenario 2*: robustness towards speed variations. To be more realistic, white noise has been added to the output joint positions in both scenarios as well as 10% of uncertainty on I_{arm}. Therefore, the robot dynamic model and the one used in the adaptive feedforward term of the controllers are not exactly the same.

Scenario 1 (S1) - Robustness towards payload changes: This scenario has been performed with 4.2 G as maximum acceleration. It is the smallest value that allows the robot to throw an object outside of its workspace. Eight different objects have been considered for this P&T task. The red lines in Fig. 2 correspond to the trajectory portions where the robot carries a payload, while the green lines represent the portions after the release point where the robot is moving without a payload. The 1^{st} and 5^{th} objects located at $\mathbf{P_1}$ and $\mathbf{P_5}$, respectively, are of 50 g of mass, the 2^{nd} and 6^{th} objects located at $\mathbf{P_2}$ and $\mathbf{P_6}$, respectively, have a mass of 100 g (i.e. $\Delta_{mass} = +100\,\%$ w.r.t the 1^{st} object), the 3^{rd} and 7^{th} objects at $\mathbf{P_3}$ and $\mathbf{P_7}$, respectively, have a mass of 150 g (i.e. $\Delta_{mass} = +200\,\%$ w.r.t the 1^{st} object), while the 4^{th} and 8^{th} ones located at $\mathbf{P_4}$ and $\mathbf{P_8}$, respectively, are of 200 g of mass (i.e. $\Delta_{mass} = +300\,\%$ w.r.t the 1^{st} object).
The Cartesian tracking errors for all the controllers are plotted in Fig. 3. It is clearly shown that the proposed controller outperforms the other controllers especially for z-axis. This can validate the robustness of the proposed RDCAL-AG controller, towards the effect of gravity, compared to the others controllers. The RMSE performance indices, in both Cartesian and joint spaces, are evaluated for all controllers and the obtained results are summarized in Table 3. These indices show a significant improvement of 44.4 % in Cartesian space and 46.3 % in joint space w.r.t to DCAL. While compared to ARISE, the indices show an improvement of 38.6 % and 18.8 % in Cartesian and joint spaces, respectively.
The evolution of the estimated parameter $\hat{m}_{tp}$, initialized to zero, is displayed in Fig. 4. It is worth to note that this mass includes both the mass of the carried payload and the mobile platform. This explains why the adaptive mass increases or returns to its nominal value depending on whether the robot is carrying a payload.
Fig. 5 illustrates the evolution of the adaptive gains, $\Lambda_p(t)$ and $\Lambda_v(t)$, versus time. One can observe, on the left side of Fig. 5, that the minimum value of $\Lambda_p(t)$ is 1135 as defined in the value of Λ_{pm}; similarly, on the right side of Fig. 5, the minimum value taken by $\Lambda_v(t)$ is the one as established in Λ_{vm}. Besides, it can be seen from this figure that, $\Lambda_p(t)$ can reach values of up to 5000 while $\Lambda_v(t)$ reaches 23.5.
The evolution of the control input torques is depicted in Fig. 6. The control signals show, for all controllers, a good and smooth behavior within the admissible limits of the actuators of the robot (the maximum torque generated by the actuators of the T3KR robot is 28.9 N.m).
As a result, this scenario demonstrates the superiority of the proposed controller over the standard DCAL and ARISE controllers. The RDCAL-AG control scheme is more robust towards variations in payload, thus, it is more suitable for P&T applications.

Scenario 2 (S2) - Robustness towards speed variations: In this scenario, the operating acceleration of the robot end-effector is increased up to 9 G following the same P&T reference trajectories described above. The objective of this scenario is to evaluate the performance of the proposed control solution for high-speed motions, where the nonlinear effects of the parallel manipulator increase substantially. In this scenario, the robot carries the same objects used in the previous scenario. The Cartesian tracking errors for all controllers are recorded and depicted in Fig. 7. The tracking errors of the three control schemes increased notably on all translational axes. Nevertheless, the proposed controller shows noticeably better performance, compared to the others two controllers. Table 3 summarizes the evaluation of the performance indices of all controllers in this scenario. It show an improvement of 49.7 % and 50.3 % in Cartesian and joint spaces, respectively, compared to DCAL. On the other hand, the improvement w.r.t the adaptive RISE was about 28.3 % in Cartesian space and 26.7 % in joint space. Fig. fig:IsolateData.eps depicts the Cartesian tracking errors for DCAL, DCAL extended by a sliding-based term and RDCAL-AG. It is obvious that adding a sliding-based term to DCAL improves the tracking performance and its robustness. This improvement is about 8%, while the improvement of RDCAL-

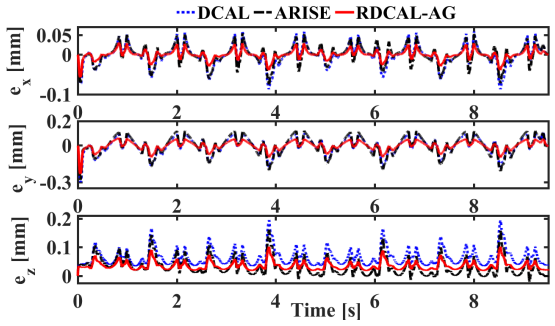

Fig. 3. Scenario 1: Evolution of the Cartesian tracking errors versus time for the tested controllers.

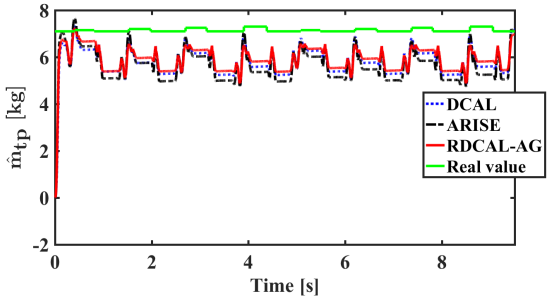

Fig. 4. Scenario 1: Evolution of the estimated mass versus time for the tested controllers.

AG over DCAL with a sliding-based term is 46%.

Fig. 8 shows the evolution of the estimated parameter $\hat{m}_{tp}$ with respect to time. The adaptation law adjusts the mass, from an initial zero value, similarly for the three controllers. We can clearly observe the oscillations induced by the changes of the payload at each pick and throw cycle.

The evolution of the adaptive gains, $\Lambda_p(t)$ and $\Lambda_v(t)$, versus time is depicted in Fig. 9. As it can be seen, the behavior of the adaptive gains $\Lambda_p(t)$ and $\Lambda_v(t)$ is slightly modified by the increase in the operating acceleration; $\Lambda_p(t)$ manages to reach values close to 6000, while $\Lambda_v(t)$ reaches values up to 24.

The control input signals for the four motors of the robot, for all the controllers, are displayed in Fig. 10. As we can see, the control signals of all the control schemes are within the allowable capacities of the motors. They are continuous and chattering-free since the sign function in the proposed controller is replaced by a continuous sigmoid function. Furthermore, it is clear that the values of the generated torques increase with the operating acceleration.

Besides, it can be noticed that the high nonlinearities and disturbances induced by the increase in the accelerations are considerably compensated by the proposed RDCAL-AG controller.

5. CONCLUSION AND FUTURE WORK

In this work, we proposed to amend the original DCAL with adaptive gains function of the system errors to counteract perturbations and uncertainties. In addition, the controller has been extended by a nonlinear sliding-based term to further improve its robustness against external disturbances. The standard DCAL, the RISE-based adaptive controller and the proposed robust DCAL with adaptive gains (RDCAL-AG) have been implemented and compared through numerical simulations on T3KR parallel robot. The obtained results clearly show the superiority of the proposed control approach compared to the

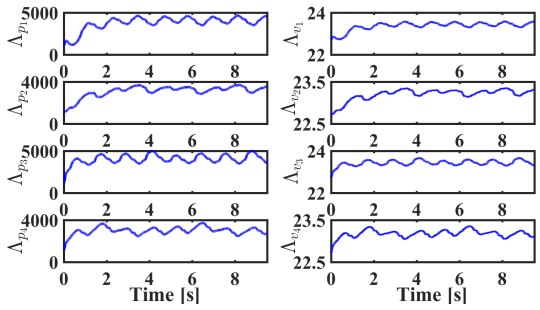

Fig. 5. Scenario 1: Evolution of the adaptive gains, $\Lambda_p(t)$ and $\Lambda_v(t)$, versus time for the proposed controller.

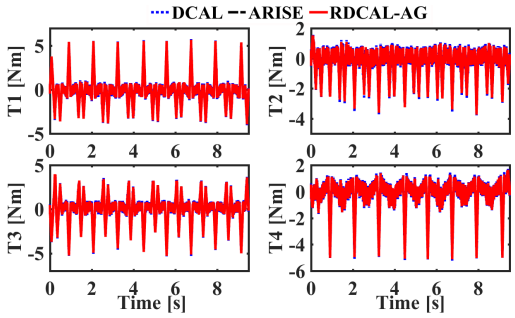

Fig. 6. Scenario 1: Evolution of the control input torques versus time for the tested controllers.

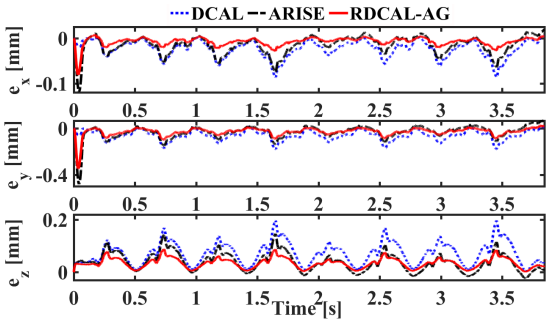

Fig. 7. Scenario 2: Evolution of the Cartesian tracking errors versus time for the tested controllers.

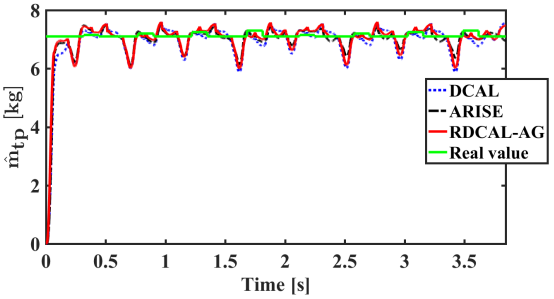

Fig. 8. Scenario 2: Evolution of the estimated mass versus time for the tested controllers.

others two controllers, in terms of tracking accuracy and robustness towards payload and velocity changes. Future directions may focus on extending this work with the stability analysis of the proposed controller as well as its validation in real-time experiments. Moreover, theoretical approaches will be considered to justify how the gain of the sliding-based term can be chosen to maximize robustness.

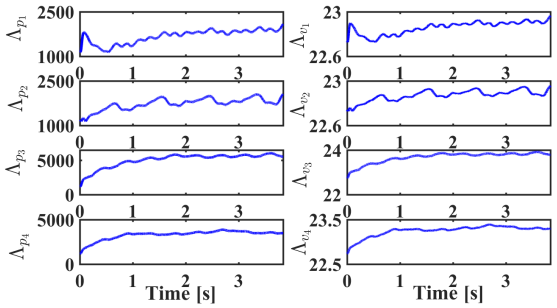

Fig. 9. Scenario 2: Evolution of the adaptive gains, $\Lambda_p(t)$ and $\Lambda_v(t)$, versus time for the proposed controller.

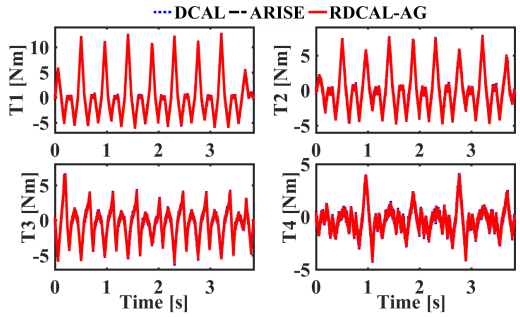

Fig. 10. Scenario 2: Evolution of the control input torques versus time for the tested controllers.

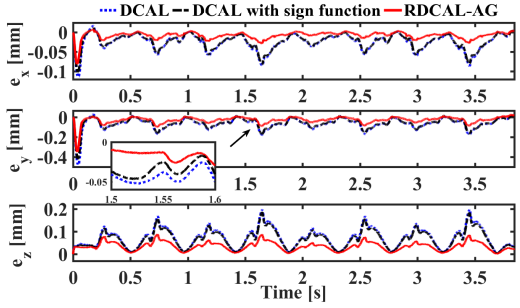

Fig. 11. Scenario 2: Evolution of the Cartesian tracking errors versus time for DCAL, DCAL with sliding-based term and RDCAL-AG controllers.

ACKNOWLEDGEMENTS

This work is supported by Tecnalia "Pick-and-Throw" research project. The corresponding author acknowledged the Lebanese University and the social foundation AZM and SAADE for financial support.

REFERENCES

Bennehar, M., Chemori, A., Bouri, M., Jenni, L.F., and Pierrot, F. (2018). A new rise-based adaptive control of pkms: design, stability analysis and experiments. *International Journal of Control*, 91(3), 593–607.

Bennehar, M., Chemori, A., and Pierrot, F. (2014). A new extension of desired compensation adaptive control and its real-time application to redundantly actuated pkms. In *2014 IEEE/RSJ International Conference on Intelligent Robots and Systems*, 1670–1675. IEEE.

Bennehar, M., Chemori, A., Pierrot, F., and Creuze, V. (2015). Extended model-based feedforward compensation in 1 adaptive control for mechanical manipulators: Design and experiments. *Frontiers in Robotics and AI*, 2, 32.

Bennehar, M., El-Ghazaly, G., Chemori, A., and Pierrot, F. (2017). A novel adaptive terminal sliding mode control for parallel manipulators: Design and real-time experiments. In *2017 IEEE International Conference on Robotics and Automation (ICRA)*, 6086–6092. IEEE.

BHS (2018). Max-AI AQC robotic sorter. `https://www.youtube.com/watch?v=2gjUpDnJrZA`.

Codourey, A. (1998). Dynamic modeling of parallel robots for computed-torque control implementation. *The International Journal of Robotics Research*, 17(12), 1325–1336.

Craig, J.J., Hsu, P., and Sastry, S.S. (1987). Adaptive control of mechanical manipulators. *The International Journal of Robotics Research*, 6(2), 16–28.

Escorcia-Hernández, J.M. (2020). *Contribution to nonlinear robust control of parallel kinematic manipulators: design and experiments*. Ph.D. thesis, Polytechnic University of Tulancingo.

Gholami, P., Aref, M., and Taghirad, H.D. (2009). Adaptive cascade control of the kntu cdrpm: a cable driven redundant parallel manipulator. In *IEEE International Conference on Robotics and Automation*.

Hassan, G., Chemori, A., Chikh, L., Hervé, P.E., El Rafei, M., Francis, C., and Pierrot, F. (2020). Rise feedback control of cable-driven parallel robots: design and real-time experiments. *IFAC-PapersOnLine*, 53(2), 8519–8524.

Honegger, M., Codourey, A., and Burdet, E. (1997). Adaptive control of the hexaglide, a 6 dof parallel manipulator. In *Proceedings of International Conference on Robotics and Automation*, volume 1, 543–548. IEEE.

Merlet, J.P. (2005). *Parallel robots*, volume 128. Springer Science & Business Media.

Natal, G.S., Chemori, A., and Pierrot, F. (2014). Dual-space control of extremely fast parallel manipulators: Payload changes and the 100g experiment. *IEEE Transactions on Control Systems Technology*, 23(4), 1520–1535.

Pi, Y. and Wang, X. (2011). Trajectory tracking control of a 6-dof hydraulic parallel robot manipulator with uncertain load disturbances. *Control Engineering Practice*, 19(2), 185–193.

Plestan, F., Shtessel, Y., Bregeault, V., and Poznyak, A. (2010). New methodologies for adaptive sliding mode control. *International journal of control*, 83(9), 1907–1919.

Sadegh, N. and Horowitz, R. (1990). Stability and robustness analysis of a class of adaptive controllers for robotic manipulators. *The International Journal of Robotics Research*, 9(3), 74–92.

Saied, H., Chemori, A., Bouri, M., El Rafei, M., Francis, C., and Pierrot, F. (2019). A new time-varying feedback rise control for second-order nonlinear mimo systems: theory and experiments. *International Journal of Control*, 1–14.

Shang, W.W., Cong, S., Li, Z.X., and Jiang, S.L. (2009). Augmented nonlinear pd controller for a redundantly actuated parallel manipulator. *Advanced Robotics*, 23(12-13), 1725–1742.

Siciliano, B., Sciavicco, L., Villani, L., and Oriolo, G. (2010). *Robotics: modelling, planning and control*. Springer Science & Business Media.

Tijjani, A.S., Chemori, A., and Creuze, V. (2020). Robust adaptive tracking control of underwater vehicles: Design, stability analysis and experiments. *IEEE/ASME Transactions on Mechatronics*.